SAE INTERNATIONAL

ARTICLE INFO
Article ID: 13-06-03-0023

doi:10.4271/13-06-03-0023

A Life Cycle Assessment of Potential Pathways to Increase Sustainable Aviation Fuel Yields through CO_2 Upgrading Co-located with Corn Ethanol Production

Stephen McCord,[1] Sam Talsma,[1] Jessey Bouchard,[2] Victor Gordillo Zavaleta,[3] Xin He,[2] and Volker Sick[1]

[1]University of Michigan-Ann Arbor, USA
[2]Aramco Americas, Aramco Research Center – Detroit, USA
[3]Aramco Europe, France

Abstract

Alcohol-to-jet (ATJ) upcycling of ethanol to sustainable aviation fuel (SAF) is an attractive emerging pathway for SAF production, especially in the US Midwest with large-scale corn ethanol production. Only 39% of the corn carbon is converted to ethanol, 20% is emitted as CO_2. Capturing the CO_2 to produce additional ethanol or SAF directly can increase the carbon yield. To guide technology selection, this work used life cycle assessment for several CO_2-to-SAF production pathways. Additionally, improvements for corn ethanol production were explored by replacing natural gas burners with heat pumps for corn drying, which reduced the carbon intensity of corn ethanol by nearly 16%. But subsequent upgrading of the ethanol to SAF is only 4.5–20% better than conventional aviation fuel. By contrast, CO_2-based alternative routes to SAF fared better, reducing carbon intensities between 83% and 90%. Gas fermentation of CO_2 to ethanol with subsequent ATJ upcycling to SAF was contrasted to Fischer–Tropsch conversion of CO_2 to SAF. Both streams require CO_2 conversion to CO, which can be produced using reverse water–gas shift or solid oxide electrolyzer cells. The Fischer–Tropsch synthesis shows a higher reduction in carbon intensity (up to 90%) compared to ATJ (up to 84.4%). For other impact categories, such as ozone depletion, ecotoxicity, and the like, the differences are of similar magnitude. Capturing CO_2 locally at the bioethanol factory and converting that CO_2 to ethanol might overall be preferable with a fermentation process that is quite like bioethanol production compared to Fischer–Tropsch synthesis for which products require a new transportation infrastructure. The aviation fuel yield from ATJ can reach 90%, higher than the 50–70% yield from Fischer–Tropsch synthesis, with gasoline and diesel fuel as major by-products for which markets will shrink in the future. Overall, ATJ appears to be the best choice for CO_2-to-SAF using the synergy with corn ethanol factories for quick launch.

History

Received: 09 Mar 2025
Revised: 12 Jun 2025
Accepted: 12 Aug 2025
e-Available: 04 Sep 2025

Keywords

Sustainable aviation fuel,
Life cycle impact analysis,
Solid oxide CO_2 electrolysis,
Alcohol-to-jet upcycling,
Fischer–Tropsch synthesis

Citation

McCord, S., Talsma, S., Bouchard, J., Zavaleta, V. et al., "A Life Cycle Assessment of Potential Pathways to Increase Sustainable Aviation Fuel Yields through CO_2 Upgrading Co-located with Corn Ethanol Production," *SAE Int. J. Sust. Trans., Energy, Env., & Policy* 6(3):199–219, 2025, doi:10.4271/13-06-03-0023.

ISSN: 2640-642X
e-ISSN: 2640-6438

This article is part of a focus issue on Low-Carbon Fuels for Sustainable Transport.

Introduction

Aviation accounts for over 1 Gt of fossil CO_2 emissions annually, approximately 2–2.5% of all anthropogenic carbon emissions [1]. As demand for aviation continues to grow, particularly for passenger services, there is a risk that the total emissions associated with the industry could continue to grow—with estimates reaching as high as 1800 Mt of CO_2 or 3500 Mt CO_2 eq. by 2050 in future travel scenarios that see increased passenger and/or freight demand without a reduction (or without sufficient reduction) in per tkm or pkm GHG emissions and thus remain "carbon intensive" [2]. While the CO_2 eq. intensity of fuels has remained largely the same since 1990, the energy intensity of travel has decreased significantly—dropping by over 50%. Clearly, there is an urgent need to decrease overall greenhouse gas (GHG) emissions in a growth sector, and net zero goals have already been set by those in the industry such as the International Air Transport Association (IATA).

One critical area for improvement in aviation is sourcing alternative, non-fossil fuels to reduce greenhouse gas (GHG) emissions and enhance sustainability and efficiency. While hydrogen-powered and electric aircraft are under development, immediate intervention is needed to meet existing goals and infrastructure demands [3]. Sustainable aviation fuel (SAF) produced from non-fossil carbon stocks offers a promising alternative to conventional jet fuel. Currently, by regulations set by fuel standards, SAF can only be used in a blend with traditional kerosene, but future developments aim for 100% SAF usage, which this study considers. SAF production is rapidly increasing, with 500 kt produced in 2023, and projections of 1500 kt for 2024—a threefold increase [4]. The hydrotreated esters and fatty acids (HEFA) pathway dominates current SAF production, but alternatives such as alcohol to jet (ATJ) are in early deployment stages. With the International Air Transport Association (IATA) setting goals for 13 Mt of SAF production annually by 2030, a nearly 10-fold increase from today, other production routes are actively being explored [5]. The US Department of Energy's Clean Fuels and Products Shot also called for ambitious goals to achieve 100% SAF compliance by 2050 [6]. Despite some concerns about cost and feedstock, embracing SAF is crucial for mitigating climate change and ensuring a sustainable future for aviation.

The utilization of CO_2 as a carbon feedstock is one such broad pathway for additional SAF production. Efforts to utilize CO_2 for SAF production are already underway at varying scales and development levels in various countries [7–13]. A key challenge that remains for rapidly deploying CO_2 to SAF pathways is the provision of sufficient biogenic CO_2 for the large-scale production of SAF. Capturing CO_2 directly from air, or from the ocean, remains limited in scale currently and faces both technological and economical challenges. With this in mind, this article describes lifecycle impacts to explore the feasibility of using the CO_2 by-product from corn ethanol fermentation as a carbon source for SAF production within the United States. Life cycle assessment (LCA) is an established approach to identify and quantify environmental risks and opportunities of production technologies. Particular emphasis is on ensuring correct accounting for how CO_2 is treated in the assessment, which otherwise often leads to wrong results of an LCA [14].

Ethanol production in the United States in 2023 amounted to 15.6 billion US gallons, producing approximately 48 Mt of CO_2—equivalent to 13 Mt of carbon, or enough carbon to meet the IATA 2030 SAF goal alone. While it is not feasible to use all this CO_2 for SAF production, it does provide a potentially useful starting point to catalyze SAF production at scale. Further, upgrading the CO_2 emissions from bioethanol production to additional ethanol for ATJ offers the chance to enhance carbon efficiency, in terms of field-to-fuel carbon percentage, helping to alleviate some of the limitations of biofuels as potential fossil replacements. At present, only 39% of the corn carbon ends up as ethanol and 20% are emitted as unused CO_2.

It should be noted that there are two promising pathways to upgrade CO_2 to SAF. Next to the ATJ route that will be the focus of this work, a comparison to the more advanced Fischer–Tropsch synthesis (FTS) is useful too in this context. For this work, both pathways to use CO_2 from corn ethanol production are analyzed to determine their life cycle impacts. Additionally, alternative means to reduce the CO_2 eq. burden of corn production is also examined here. For brevity, details of that analysis are provided in Appendix A. It is emphasized that other life cycle impacts, beyond CO_2 equivalent, are included here to investigate the broader environmental impact and to check for the undesired shifting of global warming burdens into other impact categories. In aggregate, the results of this work are expected to provide new insights into the life cycle impact to help answer whether SAF production using biogenic CO_2 from bioethanol fermentation is a sensible technology pathway and whose specific processes are most promising.

This study is focused on technical feasibility and life cycle impacts, but does not address and quantify economic and societal factors that support co-located CO_2 capture and conversion to ethanol for SAF production at bioethanol fermentation plants. It is noted, though, that the avoidance of pipeline infrastructure is a significant advantage over collecting the CO_2 and sending it to sequestration sites based on public opinion [13] and cost. Conversely, the financial incentive for sequestration of CO_2 via 45 Q tax rebates and payments is an inhibitor for SAF production.

Product System Overview

While numerous CO_2-to-SAF pathways have been proposed [15–17], a focus is made within this study to

assess a number of these determined to be of higher technology readiness level (TRL) than some potential alternatives. The study centers around the conversion of CO_2 into SAF through two pathways: FTS and the conversion of CO_2 to ethanol via gas fermentation for upgrading in the ATJ pathway.

Both the FTS pathway and fermentation pathway require (or can utilize) the production of CO from CO_2, and to this end, two technologies for the upgrading of CO_2 to CO are assessed: high-temperature CO_2 electrolysis in a solid oxide electrolysis cell (SOEC) and the reverse water–gas shift reaction (RWGS). The following paragraphs briefly introduce the key process units that were investigated in this work. Additional details on the selection of these are provided in subsequent paragraphs.

ATJ uses a three-step process that consists of dehydration, oligomerization, and hydrogenation [18], with feedstock alcohols such as ethanol or butanol. Within this product system, only ethanol is considered here. Ethanol is produced through fermentation of either corn or syngas—the latter of which will be described in more detail within this section. Ethanol is dehydrated to ethylene, before being oligomerized to fuel-length hydrocarbons, which are hydrogenated in the final stage to saturate double bonds. Following ATJ, the hydrocarbon product mix requires separation to produce the final range of products. For ATJ, the yields of kerosene reported are as high as 90%, making the route a particularly attractive proposition in situations where other fuel hydrocarbon species (e.g., gasoline, or diesel) are not desirable for production. See Appendix B for details.

FTS is a technology that can convert syngas, a mixture of CO and H_2, into a broad range of products from fuels to petrochemicals [19–22]. The range of products will vary greatly depending on numerous factors, including reactor design [21], catalyst and promotor selection [21], and operating conditions such as temperature, pressure, and H_2/CO ratios [20, 22]. Yields of kerosene produced per kg of FTS synthetic crude vary significantly, with some recent reports suggesting as high as 60–77% of the carbon ending up in kerosene [23], with others reporting figures of around 50% [24], and even lower. Potential co-products include naphtha, gasoline, and diesel. Appendices C (PEM hydrogen production) and F (Fischer–Tropsch and reverse water–gas shift) provide additional details.

Both the gas fermentation process to produce ethanol and the FTS process either require or can utilize CO. Solid oxide electrolysis (SOE) converts CO_2 to CO at high temperatures (over 700°C), with oxygen as a by-product. A detailed overview of SOE for the production of CO can be found in the literature [25–28]. A significant advantage of SOE production of CO is the high Faradaic efficiency of the process, with virtually all of the CO_2 that reacts ending as CO. Unlike the RWGS process, no H_2 feed is required. However, the need for high temperatures during operation does provide a notable drawback. On the other hand, current low-temperature CO_2 conversion alternatives suffer from operational limitations [25]. While commercial units are available for SOE of CO_2 [29], their deployment remains somewhat limited. Other notable issues, such as stack degradation, have previously been of concern, but studies have shown sufficient long-term operability, both for single and multiple operational cycles [26]. More technical details and assumptions made are provided in Appendix D.

Reverse water–gas shift (RWGS) is a thermochemical process for the conversion of CO_2 to CO, in which CO_2 is reacted with H_2 in an endothermic, reversible reaction:

$$CO_2 + H_2 \leftrightarrow CO + H_2O\left(\Delta H^{\circ}_{298K} = 41.2\,\text{kJ/mol}\right) \quad (1)$$

RWGS requires high-purity CO_2, and the reaction needs H_2 along with a catalyst material for conversion. Details on this can be found in Appendix F. H_2 is usually provided through PEM electrolysis as detailed above.

The microbial fermentation of carbon-containing gas species, primarily CO, to produce ethanol is a technology pathway that has already been commercialized on a limited scale [30]. Gas fermentation can result in the production of numerous products. However, only ethanol is within the scope of this study, although a small amount of acetic acid is also produced as a by-product for recycling or purge. A generalized equation for this can be presented as follows [31]:

$$CO + CO_2 + \left(nCO + \left(5 - n\right)H_2\right) \rightarrow CH_3CH_2OH + nCO_2 + \left(2 - n\right)H_2O \quad (2)$$

where $5 \geq n \geq -1$.

Thus, the main inputs for consideration are CO, CO_2, and H_2. The sources show a competing set of reactions as part of the Wood–Ljungdahl pathway, dependent on conditions the following can occur:

- CO can be both an energy source and a source of carbon, with acetate and ethanol produced through reactions of CO with H_2 [31–33].
- CO and H_2 can react, with both being energy sources and CO being a source of carbon to produce acetate and ethanol.
- CO_2 can be a source of carbon, with H_2 being the source of energy to produce both acetate and ethanol.

Daniell et al. stated that thermodynamically CO is favored for electron production over H_2; therefore, at high CO concentrations, hydrogenases are reversibly inhibited by CO [33]. This means that at high CO concentrations little to no H_2 uptake will occur—this will change as CO concentration drops. Although it should be noted that research into mixed microbial substrate (in place of a monoculture) research is

ongoing with the intent of finding combinations that maximize CO, CO_2, and H_2 uptake [34].

Life Cycle Assessment

The goal of this life cycle assessment is to evaluate the feasibility of producing SAF from the biogenic CO_2 by-product from corn fermentation to produce ethanol. This is a high-level, "horizon scanning"-type life cycle assessment that aims to examine the feasibility of selected technologies for the production of SAF with a focus on immediate (1 to 2 years) deployment within the United States. The study looks to characterize impacts in the production of fuels, to highlight hotspots and compare across the assessed pathways and an identified baseline, with a particular focus on the latter in terms of global warming impact.

The scope of the assessment considers the production of SAF on a cradle-to-gate basis, with no consideration included for the transport of SAF or any impacts related to its combustion. As such, no comparisons are made to the production of kerosene through traditional fossil fuel routes. Instead, to provide a baseline, the impacts of corn on SAF via the ATJ pathway are also calculated.

It is critically important to note that the results of an LCA are specific to the process studied, the assumptions made, and the rationale and choices for those need to be justified and documented. This is done for the present work within the text as well as several appendices. Background data for inputs into the system is taken from the ecoinvent 3.9 database and the DATASMART LCI package, using the cut-off by classification approach [35]. Impacts are characterized using the TRACI 2.1 method, due to the target deployment location being North American [36]. Allocation of impacts within the product system across the co-products is handled on an energy content basis of the fuels produced. Process data for the foreground is taken from a combination of literature sources, which are identified within the data inventory itself. The SOE and the gas fermentation process units were modeled here, with details of the approach to both available in the appendices.

The product system of interest is outlined in Figure 1, with the CO_2 produced from corn fermentation being the source of carbon for the downstream conversion processes. All the impacts of corn production are allocated to the ethanol and CO_2 is assumed to be a burden-free by-product. This assumption is fundamental and generally employed in LCA practices since allocation of corn production emissions to CO_2 would change the results of this study [14]. Two decision points are raised, specifically addressing how to produce CO and how to upgrade that CO into SAF.

CO_2 can be converted to CO with electrolysis cells or using RWGS reactors. In the cases presented within this study, RWGS is only considered for FTS, and not the gas fermentation route. This builds on FTS being a highly exothermic process, and the heat from this can be integrated and used synergistically for RWGS, which is an endothermic process. The lack of this heat source for fermentation greatly reduces the economic and environmental viability of using RWGS. It should be noted that the high-temperature SOE route also requires the provision of heat, but the impact of the Joule effect from cell operation helps to reduce the burden from that. To summarize, while SOE and RWGS could be used to produce the reactants for SAF production, the above explains why this work considers only the paths shown in Figure 1.

FIGURE 1 Schematic of the assessed product system.

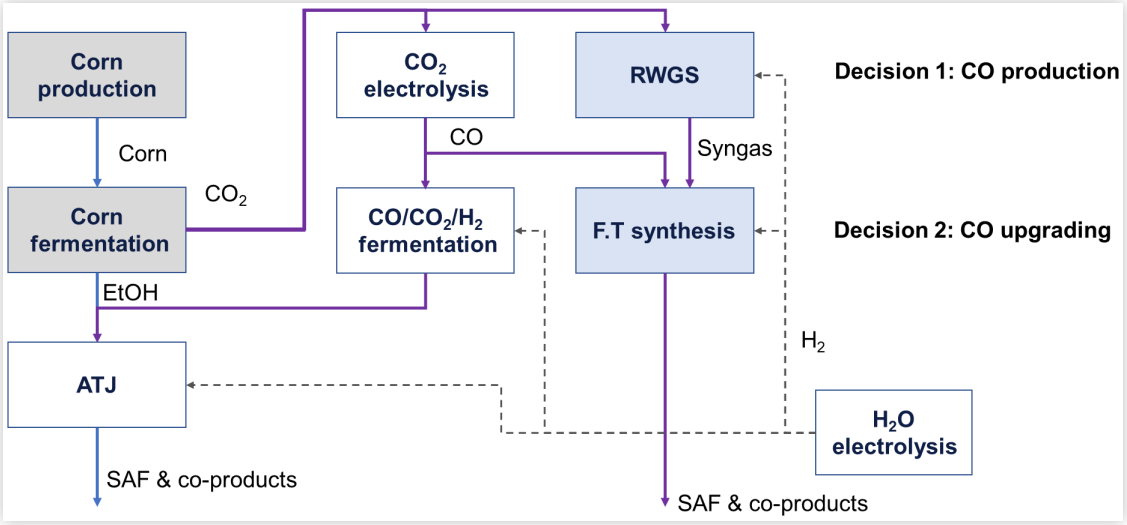

Life Cycle Inventory Overview

Detailed inventories for processes within the product system can be found in the supplementary information that is provided in Appendices A–G. The inventories for corn production and corn fermentation were taken directly from the DATASMART LCI package, with some minor modifications in the production phase. These modifications center around changes made to the corn/maize drying process, where a renewably powered industrial heat pump is considered in place of a fossil fuel–fed dryer to reduce GHG emissions by 22%.

The ATJ unit is modeled as a stand-alone process, capable of taking ethanol from either the corn or gas fermenter route, with the inventory used based on the work of Han et al. [37], with some approximations made for the relevant catalyst materials. The product mass ratio is taken to be 1:0.2:0.11 for SAF, gasoline, and diesel, respectively.

A small amount of hydrogen (approximately 3 g/kg SAF produced) is required, and for this PEM electrolysis powered by onshore wind is considered. The PEM stack and balance of plant (BoP) for the PEM electrolyzer at a 1 MW/stack scale are based on the work of Bareiß et al. [38]. Operational impacts, including normalization of the stack and BoP on a per kg H_2 basis with a lifetime of 5 and 20 years, respectively, are also included—electricity consumption for the model is taken to be 45 kWh/kg H_2 for the PEM system [39]. This same model and inventory are also used across all production stages that require H_2 provision (e.g., the FTS pathways, syngas fermentation).

For the RWGS-FTS route, an inventory was built from two sources. See Appendix F for details. The bulk of the inventory is derived from Zang et al. [40], with additional information on catalysts and water use collected separately from Rojas-Michaga et al. [41]. A product mass ratio of 1:0.55:0.59 for SAF, naphtha, and diesel, respectively, is used for outputs.

Where the RWGS-FTS inventory integrates the two stages into a single inventory, a stand-alone inventory for FTS is used for the SOE-FTS pathway. This inventory is drawn from Zang et al. and Rojas-Michaga et al. [40, 41] and results in a different product ratio of 1:0.59:0.59 for SAF, naphtha, and diesel, respectively.

For SOE, a number of inventories were derived from a combination of process modeling and literature sources. For the stack and BoP, literature sources are used to provide the input material and energy requirements [42, 43]. With respect to operational performance, two alternatives are put forward: "standard" and "advanced" scenarios in which a number of key performance parameters are used as the basis for determining operational material and energy needs. These parameters are taken from [44] and represent an estimation for the current and future performance of the SOE, with these summarized in Table 1. More details can be found in Appendix D.

TABLE 1 Key parameters used for two performance scenarios for solid oxide electrolysis.

Key parameter	Unit	Standard	Advanced
Current density	mA/cm^2	772	2500
Operational voltage (at 720°C)	V	1.41	1.3
Faradaic efficiency	%	99.5	99.5
Single pass conversion	%	65	90
Energy efficiency	%	73.1	78.1

In all scenarios modeled, heat and electricity are required inputs. Two alternatives are considered, one an expected "worst-case" baseline with heat provided from the combustion of natural gas and the second an advanced scenario where heat from biowaste incineration is considered as a lower-carbon intensity proxy.

An electrical power consumption (EPC) per Nm^3 can then be calculated for the stack—in this case, 3.7 kWh/Nm^3 for the standard case and 3.4 kWh/Nm^3 for the advanced scenario. Küngas also provides an equation to calculate the EPC, which was used as a balance check for the model as described [26]. Setting the voltage in the EPC equation at the equilibrium voltage results in a value of 2.4 kWh/Nm^3. The EPC figures for the standard and advanced models used are in a similar range to those reported by Küngas et al. [26], and the advanced figure is similar to the stack consumption in a recent ISPT report that discusses an Air Liquide CO_2 to CO use case [45].

Gas fermentation is modeled on a black box basis with a simplified reaction scheme focusing on the production of ethanol and acetate (specifically in the form of acetic acid) as a by-product, with a reaction scheme and conversion ratios based on Biermann et al. and Pardo-Planas et al. [46, 47]. Two scenarios are considered, based on the input feeds from the SOE, mirrored with the same "standard" and "advanced" nomenclature. Here, the SOE feed is assumed to be treated as a single pass, with the resultant CO–CO_2 gas mix fed to the fermentation unit.

Within the fermentation pathway, CO is preferentially used when at sufficiently high concentrations and only after this, H_2 is consumed in notable quantities [33]. H_2 is only added to convert any CO_2 present in ethanol and should only be added if the conversion is assumed to be sufficiently high both energetically and economically. It is assumed that only 50% of the CO_2 in the feed is reacted. It should be noted that the fermentation of CO_2 is also of a lower TRL than that of CO only [31, 32].

In this model, a 90% conversion of both CO and H_2 is assumed—with the remaining unreacted gases combusted before release. 5% of the product is assumed to be acetate that will be removed during distillation and returned or purged. A nutrient mix is required for operation; here, 8 g of this mix per kg of ethanol are used, using data from Lee et al. as a basis, assuming calcium chloride and ammonia make up the mix (50% mass ratio) [48].

The separation of ethanol from the fermentation broth uses the figures outlined by Jankovic et al., and adds 3 MJ of heat and 0.2 kWh of electricity demand [49].

Life Cycle Assessment Results and Discussion

A number of pathways were investigated as part of the study, combining the standard and advanced scenarios for the SOE process. The results presented in Figure 2 and Table 2 show the global warming impact related to the production of SAF across a range of pathway options. A baseline for comparison is provided through the conversion of corn ethanol to SAF through the ATJ process, with both the "default" LCI for corn ethanol and the modified version where the corn is dried with heat from heat pumps instead of from burning natural gas. SAF from ethanol that is fermented from traditionally grown and processed corn reduces the global warming potential by only 4.4% down to 80.3 g/CO_{2e}/MJ, compared to conventional jet fuel with 84 g/CO_{2e}/MJ [15]. The impact of changing the heat source is notable in the results, with a 15.6% reduction in global warming is recorded.

All investigated pathways that produce ethanol from CO_2 that was captured at the bio fermenters show a reduction in the global warming potential of 83–91%. In other words, all SAF production pathways that were investigated here lead to lower burdens compared to conventional fuel.

It should be noted that these results for corn ethanol to SAF found in the literature vary greatly—with some figures dropping to below 50 g CO_2 eq./MJ of SAF [50–54]. However, even accounting for this variation, the results presented for the CO_2 to SAF routes are lower. The impact of this is included in Figure 2, where the high-, median-, and low-carbon footprint for corn ethanol production from Scully et al. [55] is used as a basis for an additional ATJ global warming impact estimation. The three dotted horizontal lines in Figure 2 show the range of results and clearly demonstrate that even the best case for bioethanol to SAF production cannot compete with the other pathways that were assessed in this work.

The lowest figures presented relate to the SOE to FTS route using the advanced scenario combined with the lower GHG impact heat source. In the same range of 7.5–9.5 g CO_2 eq./MJ SAF are the RWGS-FTS and the SOE with natural gas to FTS routes. These results warrant a more detailed modeling approach, with this highlighted as an area of future work.

Of the CO_2 to SAF routes, the syngas fermentation routes have the highest carbon burdens. But these burdens are still only a fraction of those for traditional corn fermentation followed by FTS or ATJ, even when taking the more optimistic of the corn ethanol production scenarios.

Key contributions to, and the sensitivities of, the results to the input parameters across the different

FIGURE 2 Global warming impact results for all assessed scenarios. The lines represent equivalent results if the global warming impact of corn ethanol was taken from Scully et al. [55] to demonstrate how even lower estimates for the global warming impact of corn ethanol would result in higher carbon intensities when compared to the burden-free CO_2 routes. Vertical lines on the bars indicate uncertainty ranges.

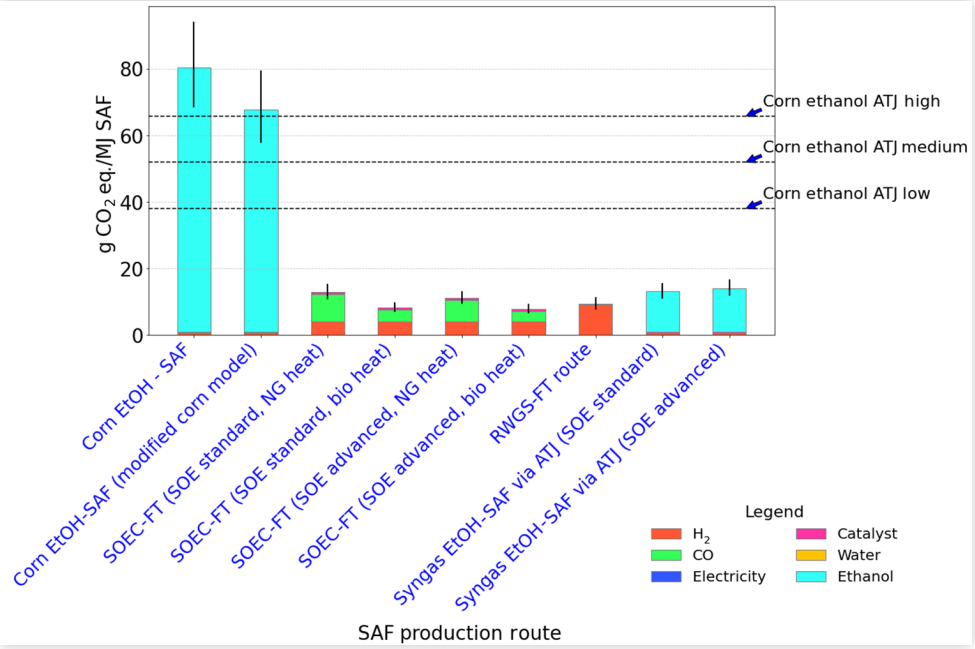

TABLE 2 Summary of the cradle-to-gate global warming results for all assessed scenarios.

SAF production route (cradle to gate)	SAF impact (kg CO_{2e}/kg SAF)	SAF impact (g CO_{2e}/MJ)
Corn ethanol to SAF through ATJ (non-modified corn production)	3.71	80.3
Corn ethanol to SAF through ATJ (modified corn production)	3.13	67.8
SAF from electrolysis to FT (standard scenario, natural gas)	0.59	12.8
SAF from electrolysis to FT (standard scenario, bio-heat)	0.38	8.2
SAF from electrolysis to FT (advanced scenario, natural gas)	0.51	11.1
SAF from electrolysis to FT (advanced scenario, bio-heat)	0.36	7.7
SAF from RWGS-FT route	0.43	9.3
Syngas ethanol to SAF through ATJ (SOEC standard, bio-heat)	0.60	13.1
Syngas ethanol to SAF through ATJ (SOEC advanced, bio-heat)	0.64	13.9

production routes are broadly determined by their contribution to the overall global warming profile, as shown in Figure 2.

For ATJ routes, impacts related to the production of ethanol are the dominant driver of impact, with minimal impacts from other parts of the inventory. As described in Appendix A, for corn ethanol, the major contributors include the drying of corn, the production of fertilizers, and the release of N_2O directly in the field. This falls broadly in line with other publications that consider bioethanol production [50, 55].

For syngas ethanol, the production of H_2 and CO are dominant factors for global warming impact. This is as expected, as the production of H_2 and CO is energetically intensive steps, either directly (HT-SOEC for CO, PEM for H_2) or indirectly (CO_2 reduction to CO using electrolytic H_2).

For CO production via SOE, the contribution to the overall impact shows the biggest variance when changing the heat source, as shown in Figure 3, where the shift from a fossil fuel source to a bio-heat source significantly reduces the global warming impact.

The performance of the SOE process stage is a major driver in many of the scenarios assessed above, for both the FTS and ATJ pathways. Figure 2 shows that the impact of changing the heat source is greater than that of the switch from the standard to the advanced scenario, and Figure 3 is included to further demonstrate the importance of using a low fossil carbon heat source. In Figure 3, the contributions of $CO_{2eq.}$ emissions to both the global warming and fossil fuel depletion impact categories are presented for three scenarios on a per kg of CO basis:

- the standard SOE with natural gas (NG) as a heat source,
- the advanced SOE with NG, and
- bio-based heat.

There is a larger reduction when changing the heat source from burning natural gas to burning biomass compared to improving a technology, i.e., going from a standard technology to an advanced version. This suggests, at least within the bounds of this study, that the scenario of deployment is arguably of greater importance than further improvement of the technology with respect to its environmental performance (notably, this does not account for the need for improved engineering performance in general).

Given the importance of heat, there is a clear need to consider the source of heat and to explore the feasibility of heat integration to further reduce this burden. For the syngas fermentation route, there is the potential to recover heat from the product gas stream before it enters the fermenter, which operates at temperatures in the range of 25–40°C. For the FTS route, the exothermic FTS reaction that operates at a significantly lower temperature of 200–350°C also provides potential for heat recovery.

When considering heat integration to further reduce external heat demand and associated impact, this would further push the relevance of the electricity contribution higher, as illustrated in Figure 3. The assessment here used wind electricity, which represents a best case for electricity, with the caveat that any carbon intensity increases from switching sources will increase the contribution to the overall total. The baseline natural gas heating scenario has the highest global warming and fossil fuel depletion impact, followed by an improved natural gas approach with heat integration. In the bio-heat scenario shown in Figure 3, it can already be seen that the electricity contribution is dominant, so any increase here would just further grow this contribution percentage.

The electricity demand differs by approximately 10% between the advanced and standard scenarios, but with little variance in the contribution from electricity. This is because the scenarios assessed only consider wind-derived electricity, which has a lower global warming impact than most alternatives. For alternatives, such as electricity taken from the US grid mix or solar PV, a decrease in electricity consumption compared to the advanced scenario would result in a higher sensitivity for global warming and fossil fuel depletion.

Changes of ±10% to the material demands of the stack or balance of plant show little sensitivity—with results varying by less than 1% of the CO total profile, and significantly less than this for the SAF profile. Decreasing the stack lifetime also shows limited sensitivity on the overall SAF global warming impact profile.

FIGURE 3 The choice of heat source for the solid oxide electrolyzer has major impact on the total global warming potential.

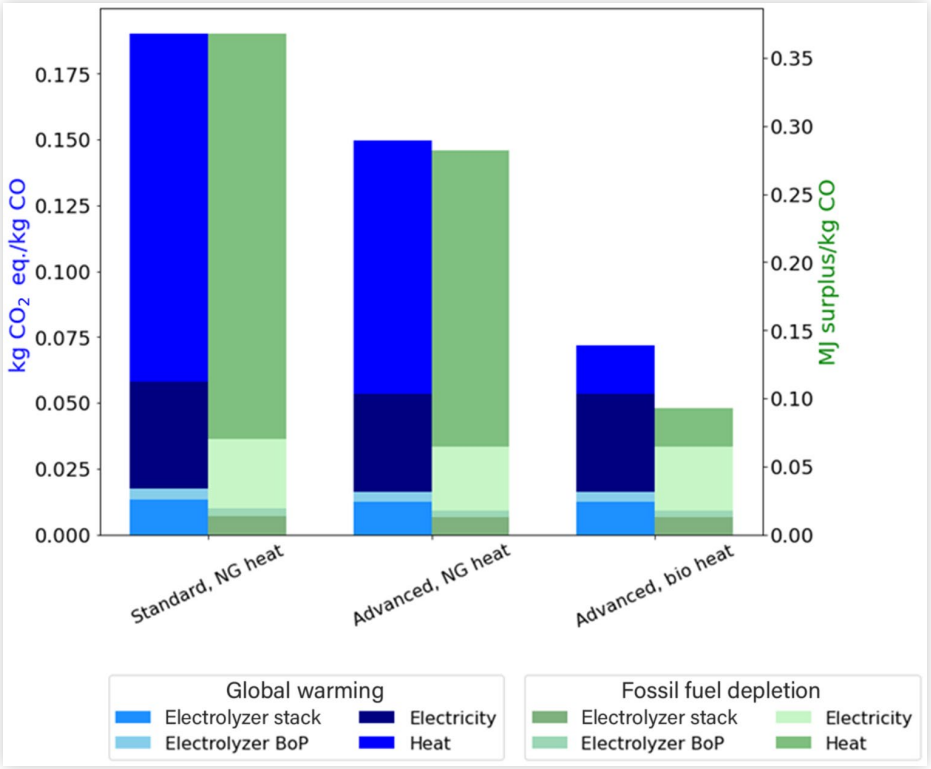

For H_2 production, electricity is the dominant contributor to the overall global warming impact profile, as shown in Figure 4. As with CO, the power source considered is wind, and any other alternative would only result in an increased contribution. As with CO production through HT-SOEC, varying the stack lifetime by 10% (from 50,000 h as a base figure) shows a ±1.5% change for the overall H_2 global warming impact profile.

From the above, the largest contributions and sensitivities within the system are derived from the sources of heat and electricity selected, and the quantities of these required to produce SAF.

Uncertainty was assessed using the pedigree matrix found in the ecoinvent database, which was later refined [56–58]. Table H.1 (in Appendix H) shows a compilation of scores for five categories (reliability, completeness, temporal correlation, geographical correlation, and further technological correlation). The results of this assessment are shown in Figure 2, where the uncertainty is represented as the error bar on each route.

The present results compare well with other published work. Where similar production pathways have been described, the results obtained in the present study qualitatively compare very well with work presented by Grim et al. [15] Minor quantitative differences are based on different databases for life cycle inventories between the two studies. Overall conclusions about CO_2-to-SAF, SAF being the best option, are not affected by these differences. Furthermore, additional cases that were examined by Grim et al. included CO_2 from other sources, such as obtained from direct air capture or even cement factories. Their results show that the global warming potential of SAF is lower than that from bioethanol, even when CO_2 is not considered burden free, as is the case for CO_2 from bio fermenters, which was one of the assumptions that was also used in the present study.

FIGURE 4 Electricity dominates the global warming impact of hydrogen production with PEM electrolysis.

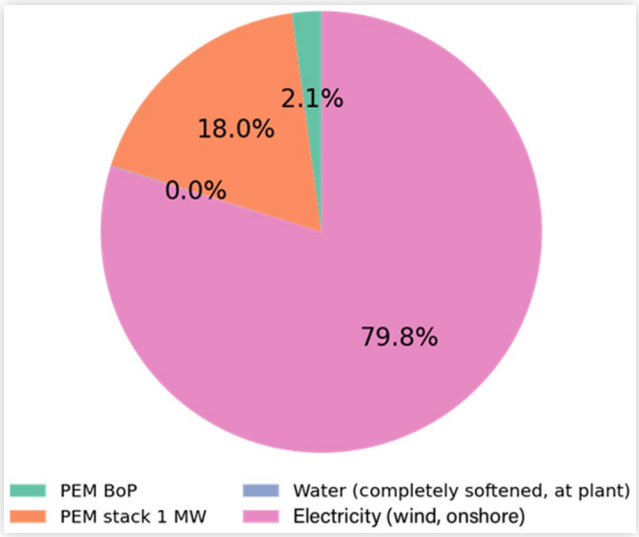

For the RWGS-FTS route the biggest contributors to global warming are unsurprisingly electricity (97% of the total is from H_2 production, and 80% of that is related to electricity), a well-documented finding in the literature. For fermentation of syngas, the picture is interesting—when it's mainly CO (in the advanced scenario), about 72% of the global warming impact is from CO, when there is more CO_2, the impact related to producing H_2 increases (contributions of 46% CO, 35% H_2 production).

It is worth mentioning that the production of CO_2 as a by-product is a secondary issue with fermentation when mainly using CO (which is closer to market or at a market solution). This can be problematic if the overall field-to-fuel carbon efficiency is of greater importance, although capture and recycle can help with this—albeit with an additional economic and environmental penalty. Given that the life cycle assessment results for RWGS and for SOE are comparable, choosing SOE as the preferred path might be an advantage due to the increased modularity of the system.

Overall, this work predominantly focused on the global warming impact category, but it is noted that other impact categories have been examined and are summarized for the different SAF production pathways. These results can be found in Table 3. Most results are within an order of magnitude of each other within the specific impact category. But several aspects deserve attention.

As with the $CO_{2eq.}$ values for corn ethanol-to-SAF that were highlighted in Figure 2, these pathways show substantially higher impacts for all categories over CO_2-to-SAF routes, with the exceptions of carcinogenics and non-carcinogenics, with these increases attributed to the electrolyzer stack and the production of wind energy. Of note, for syngas-to-ethanol-to SAF via ATJ, the advanced route shows marginally higher values for all impact categories. The advanced option produces more CO due to higher conversion in the SOEC, which changes the composition of gases that are fed into the fermenter with subsequent shifts in conversions.

However, the observed differences in all impact categories for all investigated CO_2-to-SAF pathways are mostly within a factor of 2 or even lower to each other. Given the horizon scanning approach taken, this is deemed to be acceptable. Overall, non-GHG emission impact categories provide no strong decision-making information to select any of the CO_2-to-SAF pathways over the others.

Conclusions

This study has systematically evaluated multiple pathways for producing sustainable aviation fuel (SAF) from CO_2, with a particular focus on the United States Midwest's potential given its established corn ethanol production infrastructure. Two primary routes were investigated: the alcohol-to-jet (ATJ) upcycling process and CO_2-based alternatives, including gas fermentation coupled with ATJ and FTS. LCA served as the tool to compare global warming potentials and other environmental impacts across these pathways, while also assessing technological synergies with current bioethanol facilities.

The analysis confirms that ATJ upcycling of corn-derived ethanol is an attractive and immediately implementable strategy. In the conventional corn ethanol route, only 39% of the corn carbon is converted into ethanol while approximately 20% is emitted as CO_2. By integrating CO_2 capture and co-located conversion of the CO_2 to ethanol or directly into SAF, the overall carbon yield can be substantially improved. Moreover, substituting natural gas burners with heat pumps for corn drying would reduce the carbon intensity of corn ethanol by nearly 16%. However, when the upgraded ethanol is processed via ATJ, the emission improvements relative to conventional aviation fuel are modest (only 4.5–20% reduction), which indicates room for further optimization in the conventional ATJ route.

In contrast, CO_2-utilization routes demonstrated significantly superior performance in terms of carbon intensity. Pathways that convert CO_2 using gas fermentation followed by ATJ, or through FTS, achieved reductions in carbon intensities ranging from 83% to as high as 90%. Both approaches rely on the conversion of CO_2 to CO, using either RWGS reactions or SOEC to produce the necessary synthesis gas. Notably, while FTS shows the highest reduction in greenhouse gas intensity (up to 90%), the practical yield of SAF is lower (between 50 and 70%), with gasoline and diesel emerging as major by-products. Given the projected contraction of markets for gasoline and diesel, these product streams may become less desirable in the long term.

In contrast, the ATJ pathway presents a more favorable product mix, with potential SAF yields reaching approximately 90%. This high yield and the compatibility with existing corn ethanol facilities, which already possess similar infrastructure for fermentation and product transport, make ATJ particularly attractive for rapid scale-up and early market entry. The combined ethanol streams can be transported to more centralized ATJ and refinery facilities that could use modified existing infrastructure. This strategy minimizes the need for new transportation infrastructure that would otherwise be required for moving heated syncrude from the FTS process.

Despite the promising potential of the ATJ route, the evaluation highlights several areas where further work is needed. Detailed process models for both FTS and ATJ are required to fine-tune reaction parameters and optimize overall process efficiency. Further, a comprehensive Techno-Economic Analysis (TEA) must be conducted to quantify the economic feasibility and competitiveness of these pathways under real-world operating conditions. Although FTS is an established technology, the favorable product mix and integration potential of ATJ justify increased R&D efforts aimed at its enhancement.

TABLE 3 Summary of life cycle assessment results.

Scenario (all based on per kg SAF)	Ozone depletion 10^{-8} kg CFC-11 eq.	Global warming kg CO_2 eq.	Smog 10^{-2} kg O_3	Acidification 10^{-3} kg SO_2 eq.	Eutrophication 10^{-3} kg N eq.	Carcinogenics 10^{-7} CTUh	Non-carcinogenics 10^{-7} CTUh	Respiratory effects 10^{-3} kg PM2.5 eq.	Ecotoxicity CTUe	Fossil fuel depletion MJ surplus
Corn EtOH - SAF	28.7	3.71	19.7	25.0	50.4	1.13	–6.74	1.56	23.9	4.85
Corn EtOH - SAF (modified corn model)	21.6	3.14	17.9	23.7	50.2	1.16	–7.36	1.50	25.8	3.55
SOEC - FT (SOE standard, NG heat)	7.9	0.59	3.0	3.2	1.5	1.57	4.02	0.49	11.5	0.99
SOEC - FT SOE standard, bio-heat)	7.8	0.38	4.3	3.5	2.3	1.74	4.73	0.50	13.0	0.47
SOEC - FT (SOE advanced, NG heat)	7.7	0.51	2.8	3.1	1.5	1.51	3.93	0.47	11.2	0.82
SOEC - FT (SOE advanced, bio-heat)	7.6	0.36	3.8	3.3	2.0	1.64	4.44	0.48	12.3	0.44
RWGS-FT route	15.0	0.43	3.8	4.5	2.1	2.08	6.31	0.60	17.6	0.50
Syngas EtOH - SAF via ATJ (SOE standard)	9.5	0.60	7.8	5.4	4.3	2.85	7.48	0.74	19.7	0.78
Syngas EtOH - SAF via ATJ (SOE advanced)	10.2	0.66	10.2	6.1	5.4	3.11	8.52	0.77	21.8	0.87

In summary, while all CO_2-to-SAF pathways reviewed in this study offer marked improvements over standard corn ethanol-to-SAF conversion via reduced global warming potential, the ATJ process emerges as the best option for near-term deployment. Its high SAF yield, synergistic integration with existing corn ethanol facilities, and compatibility with renewable energy sources (such as wind) collectively position it as a leading candidate for rapidly ramping up SAF production. Moreover, its inherent flexibility, being agnostic to the source of CO_2, ensures that future growth is not strictly tied to the spatial limitations of corn ethanol plants. Accordingly, combined strategies that integrate ethanol production, CO_2 capture and utilization, and ATJ upcycling can effectively jumpstart the SAF industry, paving the way for a scalable and sustainable transition in aviation fuels.

Conflict of Interest

The authors affiliated with Aramco Americas and Aramco Overseas wish to disclose that they (and by extension, their parent company, Aramco) have financial interests related to the development and future production of lower-carbon sustainable aviation fuels (SAF) via a Fischer–Tropsch (FT) process. This potential future commercial activity is related to the broader field of this research. The authors from the University of Michigan declare no conflicts of interest.

Acknowledgements

This work was supported by a grant from Aramco Services Company to the University of Michigan.

Contact Information

Volker Sick
University of Michigan
Department of Mechanical Engineering
2476 G.G. Brown Laboratory, 2350 Hayward Street
Ann Arbor, MI 48109
vsick@umich.edu

Definitions/Abbreviations

ATJ - Alcohol-to-Jet conversion
BoP - Balance of Plant
EPC - Electric Power Consumption
EtOH - Ethanol
FTS - Fischer–Tropsch Synthesis
GHG - Greenhouse Gases
HEFA - Hydrotreated esters and fatty acids
LCA - Life Cycle Assessment
LCI - Life Cycle Inventory
NG - Natural Gas
PEM - Proton Exchange Membrane
RWGS - Reverse Water–Gas Shift
SAF - Sustainable Aviation Fuel
SOEC - Solid Oxide Electrolyzer Cell

References

1. Ritchie, H. and Roser, M., "What Share of Global CO_2 Emissions Come from Aviation?," *Our World in Data*, 2024, Retrieved January 2, 2025, https://ourworldindata.org/global-aviation-emissions.
2. International Energy Agency, "Aviation," 2024, Retrieved January 2, 2025, https://www.iea.org/energy-system/transport/aviation.
3. Lohawala, N. and Wen, Z.(P.), "Navigating Sustainable Skies: Challenges and Strategies for Greener Aviation," Resources for the Future, 2024.
4. IATA, "SAF Production to Triple in 2024 but More Opportunities for Diversification Needed," June 2, 2024, Retrieved January 27, 2025, https://www.iata.org/en/pressroom/2024-releases/2024-06-02-03/.
5. International Air Transport Association, "IATA Sustainable Aviation Fuel Roadmap," 1st ed., 2015.
6. Energy.gov., "Clean Fuels & Products Shot™: Alternative Sources for Carbon-Based Products," Retrieved June 12, 2024, https://www.energy.gov/eere/clean-fuels-products-shottm-alternative-sources-carbon-based-products.
7. Norsk-e-Fuel, "Projects," 2024, Retrieved July 24, 2024, https://www.norsk-e-fuel.com/projects.
8. Repsol, "Synthetic Fuels from Renewable H_2 and CO_2," 2024, Retrieved January 2, 2025, https://www.repsol.com/en/sustainability/sustainability-pillars/environment/circular-economy/our-projects/synthetic-fuels/index.cshtml.
9. Infinium, "Ultra-Low Carbon eFuels," Retrieved January 2, 2025, https://www.infiniumco.com.
10. Twelve, "The Carbon Transformation Company™," Retrieved January 2, 2025, https://www.twelve.co.
11. Air Company, "Sustainable Aviation Fuel (SAF): AIRMADE™," Retrieved January 2, 2025, https://www.aircompany.com/sustainable-aviation-fuel/.
12. LanzaJet, "Home," Retrieved January 2, 2025, https://www.lanzajet.com/.
13. National Academies of Sciences, Engineering, and Medicine, "Carbon Utilization Infrastructure, Markets,

and Research and Development: A Final Report," The National Academies Press, Washington, DC, 2024, https://doi.org/10.17226/27732.

14. Langhorst, T., McCord, S., Zimmermann, A., Müller, L. et al., "Techno-Economic Assessment & Life-Cycle Assessment Guidelines for CO_2 Utilization (Version 2)," Global CO_2 Initiative, University of Michigan, 2022, https://dx.doi.org/10.7302/4190.
15. Grim, R.G., "Electrifying the Production of Sustainable Aviation Fuel: The Risks, Economics, and Environmental Benefits of Emerging Pathways Including CO_2," *Energy Environ. Sci.* 15 (2022): 4798-4812.
16. Bernardi, A., Danaci, D., Symes, A., and Chachuat, B., "Alternative Pathways to Sustainable Aviation Fuel from CO_2 and H_2: An Enviro-Economic Assessment," in *Computer Aided Chemical Engineering*, edited by Manenti, F. and Reklaitis, G.V., Vol. 53 (Florence, Italy: Elsevier, 2024), 2149-2154, doi:https://doi.org/10.1016/B978-0-443-28824-1.50359-8.
17. Braun, M., Grimme, W., and Oesingmann, K., "Pathway to Net Zero: Reviewing Sustainable Aviation Fuels, Environmental Impacts and Pricing," *Journal of Air Transport Management* 117 (2024): 102580, doi:https://doi.org/10.1016/j.jairtraman.2024.102580.
18. Geleynse, S., Brandt, K., Garcia-Perez, M., Wolcott, M. et al., "The Alcohol-to-Jet Conversion Pathway for Drop-In Biofuels: Techno-Economic Evaluation," *ChemSusChem* 11, no. 21 (2018): 3728-3741, doi:https://doi.org/10.1002/cssc.201801690.
19. de Klerk, A., "Chapter 10: Aviation Turbine Fuels through the Fischer–Tropsch Process," in *Biofuels for Aviation*, edited by Chuck, C.J. (Amsterdam, the Netherlands: Academic Press, 2016), 241-259, doi:https://doi.org/10.1016/B978-0-12-804568-8.00010-X.
20. Wang, W.-C., Liu, Y.-C., and Nugroho, R.A.A., "Techno-Economic Analysis of Renewable Jet Fuel Production: The Comparison between Fischer-Tropsch Synthesis and Pyrolysis," *Energy* 239 (2022): 121970, doi:https://doi.org/10.1016/j.energy.2021.121970.
21. Martinelli, M., Gnanamani, M.K., LeViness, S., Jacobs, G. et al., "An Overview of Fischer-Tropsch Synthesis: XtL Processes, Catalysts and Reactors," *Applied Catalysis A: General* 608 (2020): 117740, doi:https://doi.org/10.1016/j.apcata.2020.117740.
22. Liu, G., Yan, B., and Chen, G., "Technical Review on Jet Fuel Production," *Renewable and Sustainable Energy Reviews* 25 (2013): 59-70, doi:https://doi.org/10.1016/j.rser.2013.03.025.
23. Bube, S., Bullerdiek, N., Voß, S., and Kaltschmitt, M., "Kerosene Production from Power-Based Syngas – A Technical Comparison of the Fischer-Tropsch and Methanol Pathway," *Fuel* 366 (2024): 131269, doi:https://doi.org/10.1016/j.fuel.2024.131269.
24. Boymans, E., Nijbacker, T., Slort, D., Grootjes, S. et al., "Jet Fuel Synthesis from Syngas Using Bifunctional Cobalt-Based Catalysts," *Catalysts* 12, no. 3 (2022): 288, doi:https://doi.org/10.3390/catal12030288.
25. Detz, R.J., Ferchaud, C.J., Kalkman, A.J., Kemper, J. et al., "Electrochemical CO_2 Conversion Technologies: State-of-the-Art and Future Perspectives," *Sustainable Energy & Fuels* 7, no. 23 (2023): 5445-5472, doi:https://doi.org/10.1039/D3SE00775H.
26. Küngas, R., Blennow, P., Heiredal-Clausen, T., Nørby, T.H. et al., "Progress in SOEC Development Activities at Haldor Topsøe," *ECS Transactions* 91, no. 1 (2019): 215, doi:https://doi.org/10.1149/09101.0215ecst.
27. Küngas, R., "Review—Electrochemical CO_2 Reduction for CO Production: Comparison of Low- and High-Temperature Electrolysis Technologies," *Journal of the Electrochemical Society* 167, no. 4 (2020): 044508, doi:https://doi.org/10.1149/1945-7111/ab7099.
28. Hauch, A., Küngas, R., Blennow, P., Hansen, A.B. et al., "Recent Advances in Solid Oxide Cell Technology for Electrolysis," *Science* 370, no. 6513 (2020): eaba6118, doi:https://doi.org/10.1126/science.aba6118.
29. TOPSOE, "Produce Your Own Carbon Monoxide | CO_2 to CO | Carbon Dioxide to Carbon Monoxide | Topsoe," Retrieved July 24, 2024, https://www.topsoe.com/processes/carbon-monoxide.
30. LanzaJet, "Building the Sustainable Aviation Fuel (SAF) Industry and Catalyzing Global Production," Breakthrough Energy, 2022.
31. Phillips, J.R., Huhnke, R.L., and Atiyeh, H.K., "Syngas Fermentation: A Microbial Conversion Process of Gaseous Substrates to Various Products," *Fermentation* 3, no. 2 (2017): 28, doi:https://doi.org/10.3390/fermentation3020028.
32. Sun, X., Atiyeh, H.K., Huhnke, R.L., and Tanner, R.S., "Syngas Fermentation Process Development for Production of Biofuels and Chemicals: A Review," *Bioresource Technology Reports* 7 (2019): 100279, doi:https://doi.org/10.1016/j.biteb.2019.100279.
33. Daniell, J., Köpke, M., and Simpson, S.D., "Commercial Biomass Syngas Fermentation," *Energies* 5, no. 12 (2012): 5372-5417, doi:https://doi.org/10.3390/en5125372.
34. Grimalt-Alemany, A., Łężyk, M., Lange, L., Skiadas, I.V. et al., "Enrichment of Syngas-Converting Mixed Microbial Consortia for Ethanol Production and Thermodynamics-Based Design of Enrichment Strategies," *Biotechnology for Biofuels* 11, no. 1 (2018): 198, doi:https://doi.org/10.1186/s13068-018-1189-6.
35. Wernet, G., Bauer, C., Steubing, B., Reinhard, J. et al., "The Ecoinvent Database Version 3 (Part I): Overview and Methodology," *The International Journal of Life Cycle Assessment* 21, no. 9 (2016): 1218-1230, doi:https://doi.org/10.1007/s11367-016-1087-8.
36. Bare, J.C., "Tool for Reduction and Assessment of Chemicals and Other Environmental Impacts (TRACI), Version 2.1 - User Manual," Data and Tools, December 2015.
37. Han, J., Tao, L., and Wang, M., "Well-to-Wake Analysis of Ethanol-to-Jet and Sugar-to-Jet Pathways," *Biotechnology for Biofuels* 10, no. 1 (2017): 21, doi:https://doi.org/10.1186/s13068-017-0698-z.

38. Bareiß, K., de la Rua, C., Möckl, M., and Hamacher, T., "Life Cycle Assessment of Hydrogen from Proton Exchange Membrane Water Electrolysis in Future Energy Systems," *Applied Energy* 237 (2019): 862-872, doi:https://doi.org/10.1016/j.apenergy.2019.01.001.
39. International Renewable Energy Agency, "Making the Breakthrough: Green Hydrogen Policies and Technology Costs," Abu Dhabi, UAE, 2021.
40. Zang, G., Sun, P., Elgowainy, A., Bafana, A. et al., "Life Cycle Analysis of Electrofuels: Fischer-Tropsch Fuel Production from Hydrogen and Corn Ethanol Byproduct CO_2," *Environ Sci Technol* 55, no. 6 (2021): 3888-3897, doi:https://doi.org/10.1021/acs.est.0c05893.
41. Rojas-Michaga, M.F., Michailos, S., Cardozo, E., Akram, M. et al., "Sustainable Aviation Fuel (SAF) Production through Power-to-Liquid (PtL): A Combined Techno-Economic and Life Cycle Assessment," *Energy Conversion and Management* 292 (2023): 117427, doi:https://doi.org/10.1016/j.enconman.2023.117427.
42. Krishnan, S., Corona, B., Kramer, G.J., Junginger, M. et al., "Prospective LCA of Alkaline and PEM Electrolyser Systems," *International Journal of Hydrogen Energy* 55 (2024): 26-41, doi:https://doi.org/10.1016/j.ijhydene.2023.10.192.
43. Rillo, E., Gandiglio, M., Lanzini, A., Bobba, S. et al., "Life Cycle Assessment (LCA) of Biogas-Fed Solid Oxide Fuel Cell (SOFC) Plant," *Energy* 126 (2017): 585-602, doi:https://doi.org/10.1016/j.energy.2017.03.041.
44. Huang, Z., Grim, R.G., Schaidle, J.A., and Tao, L., "The Economic Outlook for Converting CO_2 and Electrons to Molecules," *Energy & Environmental Science* 14, no. 7 (2021): 3664-3678, doi:https://doi.org/10.1039/D0EE03525D.
45. Institute for Sustainable Process Technology, "Next Level Solid Oxide Electrolysis," August 2023.
46. Biermann, M., Montañés, R.M., Normann, F., and Johnsson, F., "Carbon Allocation in Multi-Product Steel Mills that Co-process Biogenic and Fossil Feedstocks and Adopt Carbon Capture Utilization and Storage Technologies," *Frontiers in Chemical Engineering* 2 (2020): 596279, doi:https://doi.org/10.3389/fceng.2020.596279.
47. Pardo-Planas, O., Atiyeh, H.K., Phillips, J.R., Aichele, C.P. et al., "Process Simulation of Ethanol Production from Biomass Gasification and Syngas Fermentation," *Bioresource Technology* 245 (2017): 925-932, doi:https://doi.org/10.1016/j.biortech.2017.08.193.
48. Lee, U., Hawkins, T.R., Yoo, E., Wang, M. et al., "Using Waste CO_2 from Corn Ethanol Biorefineries for Additional Ethanol Production: Life-Cycle Analysis," *Biofuels, Bioproducts and Biorefining* 15, no. 2 (2021): 468-480, doi:https://doi.org/10.1002/bbb.2175.
49. Janković, T., Straathof, A.J.J., and Kiss, A.A., "Advanced Downstream Processing of Bioethanol from Syngas Fermentation," *Separation and Purification Technology* 322 (2023): 124320, doi:https://doi.org/10.1016/j.seppur.2023.124320.
50. Lee, U., Kwon, H., Wu, M., and Wang, M., "Retrospective Analysis of the U.S. Corn Ethanol Industry for 2005–2019: Implications for Greenhouse Gas Emission Reductions," *Biofuels, Bioproducts and Biorefining* 15, no. 5 (2021): 1318-1331, doi:https://doi.org/10.1002/bbb.2225.
51. Xu, H., Lee, U., and Wang, M., "Life-Cycle Greenhouse Gas Emissions Reduction Potential for Corn Ethanol Refining in the USA," *Biofuels, Bioproducts and Biorefining* 16, no. 3 (2022): 671-681, doi:https://doi.org/10.1002/bbb.2348.
52. Rosenfeld, J., Lewandrowski, J., Hendrickson, T., Jaglo, K. et al., "A Life-Cycle Analysis of the Greenhouse Gas Emissions from Corn-Based Ethanol," Report Prepared by ICF under USDA Contract No. AG-3142-D-17-0161, September 2018.
53. Soleymani Angili, T., Grzesik, K., Rödl, A., and Kaltschmitt, M., "Life Cycle Assessment of Bioethanol Production: A Review of Feedstock, Technology and Methodology," *Energies* 14, no. 10 (2021): 2939, doi:https://doi.org/10.3390/en14102939.
54. Pereira, L.G., Cavalett, O., Bonomi, A., Zhang, Y. et al., "Comparison of Biofuel Life-Cycle GHG Emissions Assessment Tools: The Case Studies of Ethanol Produced from Sugarcane, Corn, and Wheat," *Renewable and Sustainable Energy Reviews* 110 (2019): 1-12, doi:https://doi.org/10.1016/j.rser.2019.04.043.
55. Scully, M.J., Norris, G.A., Alarcon Falconi, T.M., and MacIntosh, D.L., "Carbon Intensity of Corn Ethanol in the United States: State of the Science," *Environmental Research Letters* 16, no. 4 (2021): 043001, doi:https://doi.org/10.1088/1748-9326/abde08.
56. Ciroth, A., Muller, S., Weidema, B., and Lesage, P., "Empirically Based Uncertainty Factors for the Pedigree Matrix in Ecoinvent," *The International Journal of Life Cycle Assessment* 21, no. 9 (2016): 1338-1348, doi:https://doi.org/10.1007/s11367-013-0670-5.
57. Muller, S., Lesage, P., Ciroth, A., Mutel, C. et al., "The Application of the Pedigree Approach to the Distributions Foreseen in Ecoinvent V3," *The International Journal of Life Cycle Assessment* 21, no. 9 (2016): 1327-1337, doi:https://doi.org/10.1007/s11367-014-0759-5.
58. Heijungs, R. and Huijbregts, M.A.J., "A Review of Approaches to Treat Uncertainty in LCA," in *International Congress on Environmental Modelling and Software*, Osnabrück, Germany, 2004, https://scholarsarchive.byu.edu/iemssconference/2004/all/197.
59. Peplinski, A.J., Paulis, J.W., Bietz, J.A., and Pratt, R.C., "Drying of High-Moisture Corn: Changes in Properties and Physical Quality," *Cereal Chemistry* 71, no. 2 (1994): 129-133.
60. Altay, F. and Gunasekaran, S., "Influence of Drying Temperature, Water Content, and Heating Rate on Gelatinization of Corn Starches," *Journal of Agricultural and Food Chemistry* 54, no. 12 (2006): 4235-4245, doi:https://doi.org/10.1021/jf0527089.
61. da Silva, G.M., Ferreira, A.G., Coutinho, R.M., and Maia, C.B., "Energy and Exergy Analysis of the Drying of Corn

Grains," *Renewable Energy* 163 (2021): 1942-1950, doi:https://doi.org/10.1016/j.renene.2020.10.116.

62. Calibrate Energy Engineering, "Heat Pump Installation Installed to Dry 30,000 Tonnes of Grain," May 3, 2020, Retrieved July 25, 2024, https://www.calibrateenergy.co.uk/the-wheat-from-the-chaff/.
63. Grat Energy Inc., "Heat Pump Drying Solutions for Grain," Leading Heat Pump Manufacturers & Solutions Provider | GRAT, Retrieved July 25, 2024, https://gratpro.com/heat-pump-drying-solutions-for-grain/.
64. Ni, M., "Modeling of a Solid Oxide Electrolysis Cell for Carbon Dioxide Electrolysis," *Chemical Engineering Journal* 164, no. 1 (2010): 246-254, doi:https://doi.org/10.1016/j.cej.2010.08.032.
65. Staffell, I., Ingram, A., and Kendall, K., "Energy and Carbon Payback Times for Solid Oxide Fuel Cell Based Domestic CHP," *International Journal of Hydrogen Energy* 37, no. 3 (2012): 2509-2523, doi:https://doi.org/10.1016/j.ijhydene.2011.10.060.

Appendices

Appendix A: Corn and Ethanol Production

The LCI for the production of corn is based on the DATASMART LCI model "*Corn, at farm/US US-EI U*" with a modification made to the "*Maize drying/US* US-EI U*" inventory used within this. The inventory covers all aspects of corn production from the cultivation and harvesting of corn including drying and transport from the field to storage.

Analysis of the production of corn lifecycle shows that the major GHG emissions for corn farming relate to CO_2 and N_2O, with these remaining as major contributing factors in the global warming impact of corn bioethanol production. Within the study, three elements were identified as potential areas where GHG emissions could be reduced: the drying of the harvested corn, in-field application of fertilizer, and the emissions related to fertilizer production. Paths to GHG reductions in all three elements were explored: improving drainage for reduced N_2O, electrolysis-derived H_2 in place of steam methane reformation to produce N fertilizers, and the electrification of drying corn. However, only the electrification of corn drying is included within this assessment; this decision was made as it is deemed the easiest to implement at scale under a reasonable timescale.

Corn drying can be passive or active. Earlier in the growing season (spring or summer) drying is predominantly handled in the field, or through natural airflow systems—as discussed in the sources found at the end of the prior paragraph. As temperatures begin to drop or if corn needs to be dried more rapidly, active drying processes can be employed. Drying with heated air can occur at a range of temperatures, with this impacting the amount of time required to bring down moisture content to a level safe for storage. However, air temperatures need to remain low enough not to damage the corn [59] his generally means that temperatures are kept below 100°C [59, 60].

Currently, mechanical or active drying typically uses fossil fuels as a heat source, as reflected in the DATASMART corn model. However, alternatives to fossil fuels are an area of research interest—with alternatives such as solar dryers [61] or heat pumps provided as examples. Here, the focus is made on the latter with industrial examples already made available for purchasing and installation—covering both air source and ground source examples [62, 63].

The existing corn-to-ethanol pathway is modeled using existing DATASMART life cycle inventories, with modifications made to the corn drying activity. Here, the heat (in MJ) supplied by the burning of fossil fuels is swapped on an equal basis for the heat provided by an industrial heat pump.

The model for the heat pump is modified from the ecoinvent model "*Heat, air-water heat pump 10kW {Europe without Switzerland}| heat production, air-water heat pump 10kW | Cut-off, U*" where the electricity source is changed to the DATASMART LCI model for wind power—"*Electricity, at wind power plant 800kW/US- US-EI U*". All remaining inputs (the heat pump construction and it's normalized per MJ contribution, the amount of electricity needed to generate 1 MJ of heat) and its outputs (the amount of refrigerant output per MJ of heat) remain the same.

The flowchart in Figure A.1 maps the changes made to the models.

Appendix B: Alcohol to Jet

Modeling the conversion of ethanol to SAF on a standalone basis is built on published literature, predominantly from Han et al. [37] (Table B.1).

Appendix C: PEM Electrolysis for Hydrogen

The PEM electrolyzer balance of plant and stack inventories is taken from Bareiß et al. [38]. Results are scaled for a production of 150 t of H_2 production per year/stack (Table C.1). The electrolyzer (and therefore the balance of plant) is assumed to operate for 20 years, with stack replacements every 5 years of operation. Life cycle inventories for the balance of plant (Table S2), electrolyzer stack (Table C.2), and the operation of the plant (Table C.3) are shown below.

FIGURE A.1 Flowchart representing changes made to upstream ethanol production supply chain.

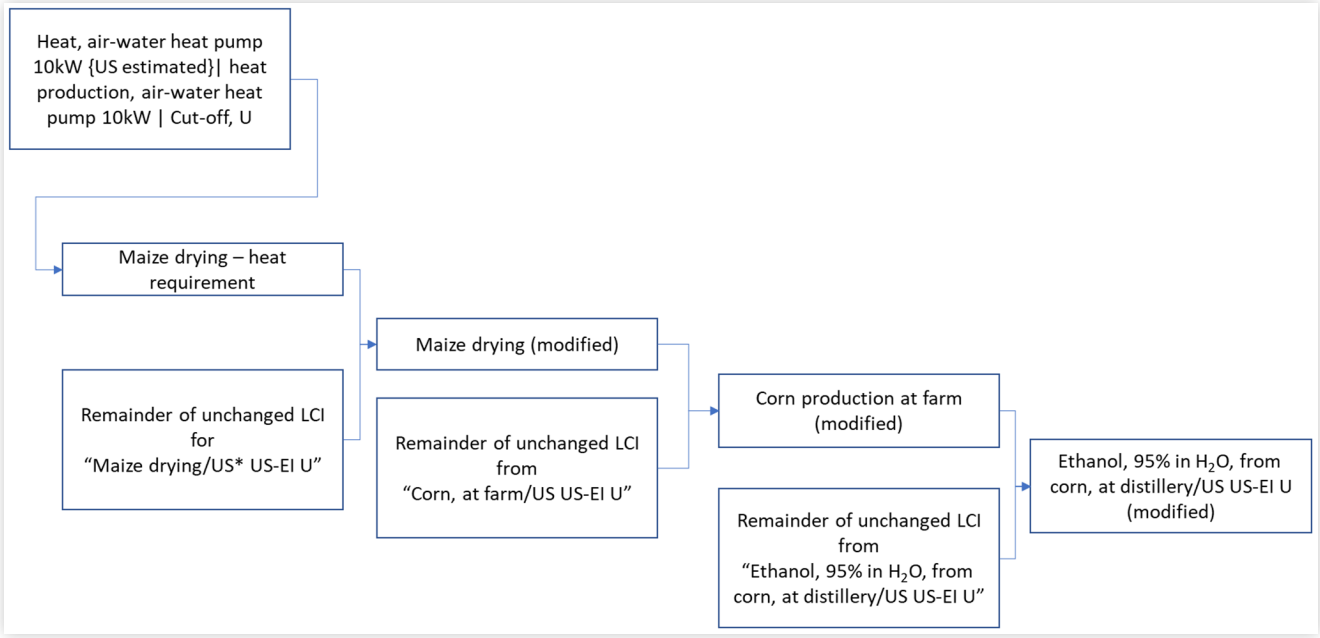

TABLE B.1 Life cycle inventory for ethanol-to-jet model.

Output	Qty	Unit
Kerosene for SAF	1	kg
Gasoline	0.2	kg
Diesel	0.11	kg
Input	**Qty.**	**Unit**
Modified model for ethanol production, based on: Ethanol, 95% in H_2O, from corn, at distillery/US US-EI U	2.38	kg
Nickel sulfate {GLO}| market for nickel sulfate | cut-off, U	3	g
Alumina, at plant NREL/US U	3	g
Hydrogen, PEM electrolysis	3	g
Electricity, at wind power plant 800 kW/US- US-EI U	1.1	kWh

TABLE C.1 Inventory for balance of plant at a 1 MW scale.

Output	Qty.	Unit
Electrolyzer Balance of Plant (1 MW)	1	p
Input	**Qty.**	**Unit**
Steel, electric, un- and low-alloyed, at plant/US-US-EI U	4800	kg
Steel, electric, chromium steel 18/8, at plant/US- US-EI U	1900	kg
Aluminum ingot, production mix, at plant NREL/US U	50	kg
Copper, at regional storage/US-US-EI U	50	kg
Polyethylene, HDPE, granulate, at plant/US-US-EI U	300	kg
Electronics for control units/US-US-EI U	1100	kg
Concrete, sole plate and foundation, at plant (2385 kg/m^3)/US*US-EI U	5600	kg

TABLE C.2 Inventory for the 1 MW stack.

Output	Qty.	Unit
Electrolyzer Stack (1 MW)	1	p
Input	**Qty.**	**Unit**
Titanium {GLO}| market for titanium | cut-off, U	528	kg
Aluminum ingot, production mix, at plant NREL/US U	27	kg
Steel, electric, chromium steel 18/8, at plant/US-US-EI U	100	kg
Copper, at regional storage/US-US-EI U	4.5	kg
Tetrafluoroethylene, at plant/US-US-EI U	16	kg
Activated carbon, granular {GLO}| market for activated carbon, granular | cut-off, U	9	kg
Platinum {GLO}| market for platinum | cut-off, U (used as proxy for iridium)	0.75	kg
Platinum {GLO}| market for platinum | cut-off, U	0.075	kg

TABLE C.3 Inventory for hydrogen production on a per kg basis.

Output	Qty.	Unit
Hydrogen	1	kg
Oxygen (vented)	8	kg
Input	**Qty.**	**Unit**
PEM balance of plant	3.33E−07	p
PEM stack 1 MW size	1.33E−06	p
Water, completely softened, at plant/US-US-EI U	12	kg
Electricity, at wind power plant 800 kW/US-US-EI U	45	kWh

Appendix D: Solid Oxide Electrolysis of CO_2

Inventories for the stack and balance of plant are adapted from Rillo et al. [43]. It is noted that the oxygen which is produced in the CO_2 electrolysis as well is considered burden-free in this analysis and is not further considered (assumed to be vented), although, as with hydrogen electrolysis, this may prove to be a valuable by-product in actual deployment scenarios.

CO_2 from the bioethanol fermentation stage is captured and fed to a solid oxide electrolysis system. A unit in the system is taken to be 4 × 250 kW stacks, mounted to a 1 MW balance of plant. The modeled output of each 250-kW stack is in the same order as those reported for the Haldor Topsoe eCOs system (stated to be 96 Nm^3/h) [26]. The plant is assumed to operate at a temperature of 720°C and convert CO_2 to CO for further processing to ethanol via fermentation or for feed into the FTS unit.

The operation of the SOEC was modeled for two scenarios, with inventories included for both. First, a "standard" scenario is taken to represent a baseline that uses current performance. Second, an "advanced" scenario is investigated that considers an improved future-predicted performance. Both scenarios draw key parameters from NREL [44]. These key parameters are summarized in Table D.1.

The equilibrium potential at 720°C was calculated using an expression provided in a solid oxide model [64]. A voltage of 1.02 V for the operational temperature represents the minimum voltage required to drive the reaction at the cathode of the cell. No calculation of the overpotential is made; instead the figures provided by Huang et al. [44] listed in Table D.1 are used.

The initial overpotential is taken to be the operational minus the equilibrium voltage. A notable issue for solid oxide electrolysis cells has been the degradation of the cells within the stack, typically resulting in an increase in resistance and the operational voltage. A degradation rate of 1.2% per 1000 h of operation is used here, as a conservative figure from Küngas et al., with this increasing the voltage required for stack operation [26]. This degradation is taken to be linear, and an average cell voltage is used in the model that accounts for the degradation over the 2-year life span of the stack.

Tables D.2–D.4 provide more details on components and life cycle inventories.

TABLE D.1 Key operational parameters of standard and advanced SOEC scenarios.

Key parameter	Unit	Standard	Advanced
Current density	mA/cm^2	772	2500
Operational voltage (at 720°C)	V	1.41	1.3
Faradaic efficiency	%	99.5	99.5
Single pass conversion	%	65	90
Energy efficiency	%	73.1	78.1

TABLE D.2 Balance-of-plant components for a 1 MW plant that includes four 250 kW stacks.

Output	Qty	Unit	
Solid oxide electrolyzer—BoP—1 MW	1	p	
Input	**Qty**	**Unit**	**Notes**
Steel, low-alloyed, at plant/US-US-EI U	12,200	kg	
Steel, electric, chromium steel 18/8, at plant/US-US-EI U	3600	kg	
Zinc oxide, at plant/US-US-EI U	4080	kg	
Iron ore concentrate {GLO}| market for iron ore concentrate | cut-off, U	3050	kg	Proxy for iron oxide
Inverter, 500 kW, at plant/US-/I US-EI U	2	p	
Metal working, average for steel product manufacturing {GLO}| market for metal working, average for steel product manufacturing | cut-off, S	15,800	kg	
Heat, natural gas, at industrial furnace >100 kW/US-US-EI U	122,000	MJ	
Electricity, high voltage, consumer mix, at grid/US US-EI U	1200	kWh	*

TABLE D.3 Life cycle inventory for one 250 kW SOEC stack.

Output	Qty	Unit	Notes
Solid oxide electrolyzer—stack—250 kW	1	p	
Input	**Qty**	**Unit**	**Notes**
Nickel oxide	150	kg	Custom module
YSZ	67	kg	Custom module
LSM	0.62	kg	Custom module
Ethanol, 95% in H_2O, from corn, at distillery/US US-EI U	28	kg	Solvent
Methyl ethyl ketone, at plant/US- US-EI U	54	kg	Solvent
Carbon black {GLO}| market for carbon black | cut-off, U	0.46	kg	
Modified starch, at plant/US-US-EI U	10.6	kg	Binder material
Ethylene glycol, at plant/US-US-EI U	9.03	kg	Binder material
Steel, converter, chromium steel 18/8, at plant/US-US-EI U	2500	kg	Interconnect
Steel, converter, chromium steel 18/8, at plant/US-US-EI U	1000	kg	Casing
Electricity, medium voltage, certified electricity, at grid/US*US-EI U	55	MWh	
Direct emissions			
Carbon dioxide	108	kg	

TABLE D.4 Life cycle inventory summary for the SOEC scenarios (per kg CO basis).

		Scenario			
Component	**Unit**	**Standard, NG**	**Standard, Bio**	**Advanced, NG**	**Advanced, Bio**
Outputs					
Carbon monoxide	kg	1	1	1	1
Carbon dioxide	kg	0.85	0.85	0.17	0.17
Oxygen (vent)	kg	0.57	0.57	0.57	0.57
Inputs					
Carbon dioxide, biogenic	kg	2.42	2.42	1.75	1.75
Solid oxide electrolyzer—stack—250 kW	P	7.13E−07	7.13E−07	6.57E−07	6.57E−07
Solid Oxide Electrolyzer—BoP—1 MW	P	3.57E−08	3.57E−08	3.29E−08	3.29E−08
Electricity, at wind power plant 800 kW/US-US-EI U	kWh	3.51	3.51	3.21	3.21
Heat, natural gas, at boiler condensing modulating >100 kW/US-US-EI U	kWh	0.48	-	0.35	-
Heat, biowaste, at waste incineration plant, allocation price/US*US-EI U	kWh	-	0.48	-	0.35

TABLE D.5 Life cycle inventory for the production of YSZ.

Output	Qty	Unit
YSZ	1	kg
Inputs	**Qty**	**Unit**
Yttrium oxide {GLO}| market for yttrium oxide | cut-off, U	0.03	kg
Zinc oxide {GLO}| market for zinc oxide | cut-off, U	0.97	kg
Urea {RNA}| market for urea | cut-off, U	0.7	kg
Water, deionized {Europe without Switzerland}| market for water, deionized | cut-off, U	4	kg
Electricity, medium voltage, certified electricity, at grid/US*US-EI U	0.95	kWh

The standard stack requires an active area of 20.9 m^2, and the advanced stack requires an area of 7 m^2, due to the increased current density, to deliver the necessary power output.

The total delivered current is determined by the current density multiplied by the active area, with this used to derive the production of CO in Nm^3/h. An electrical power consumption (EPC) per Nm^3 can then be calculated for the stack, with 3.7 kWh/Nm^3 for the standard case and 3.4 kWh/Nm^3 for the advanced case calculated.

For CO_2 electrolysis, a thermoneutral voltage of 1.47 V is reported. Substituting this into the EPC gives a figure of around 3.6 kWh/Nm—suggesting that additional heat is needed to maintain cell temperatures for the advanced scenario and for the standard scenario until degradation occurs [28]. It is assumed that this heat is provided by supplying the increased overpotential necessary to retain thermoneutral operation. It is also assumed that additional heat energy is required to raise the temperature of the incoming gases to the cell operating temperature. This was modeled by considering the average Cp value of the gas mix between an ambient temperature (25°C) and the operating temperature of 720°C to estimate a heat duty.

The source of heat has a significant impact on the results—the ISPT report includes the use of an electrical heating as a source, for example [45]. Here, two alternatives are considered in natural gas and a low fossil carbon proxy in the form of heat generated from the combustion/incineration of biomass wastes. For the standard case, heat requirements are calculated to be 0.48 kWh/kg CO, and the advanced 0.35 kWh/kg CO.

With regard to the balance of plant energy consumption, an additional 15% of energy (assumed to be totally electrical) is added to the energy requirements to bring the overall energy efficiency of the system broadly in line with the figures in the key parameters table taken from NREL. Finally, only a limited recycle stream is considered, with the main purpose of this being that a small amount of CO in the feed is considered in some sources to be beneficial for operation. See Table D.4 for details.

In Table D.3, three custom modules are used, with data taken from Staffell et al. [65]. These modules are described in Tables D.5–D.7.

TABLE D.6 Life cycle inventory for the production of nickel oxide.

Outputs	Qty	Unit
Nickel oxide	1	kg
Inputs	**Qty**	**Unit**
Air	0.5	kg
Nickel, 99.5%, at plant/GLO US-EI U	0.786	kg
Heat, central or small-scale, natural gas {RER}| market group for heat, central or small-scale, natural gas | cut-off, U	4	MJ

TABLE D.7 Life cycle inventory for the production of LSM.

Outputs	Qty	Unit
LSM	0.226	kg
Inputs	**Qty**	**Unit**
Lanthanum nitrate	0.227	kg
Strontium nitrate	0.064	kg
Manganese nitrate	0.179	kg
Glycine {GLO}| market for glycine | cut-off, U	0.3	kg
Water, deionized {Europe without Switzerland}| market for water, deionized | cut-off, U	2	kg
Electricity, medium voltage, certified electricity, at grid/US*US-EI U	3.55	kWh

In Table D.7 the nitrate compounds are also custom modules:

- 1 kg lanthanum nitrate is modeled as: 0.501 kg of lanthanum oxide [lanthanum oxide {GLO}| market for lanthanum oxide | cut-off, U], and 0.639 kg of nitric acid [nitric acid, 50% in H_2O, at plant/US-US-EI U]
- 1 kg of manganese nitrate is modeled as: 0.517 kg of nitrous dioxide [nitrous dioxide {RER}| market for nitrous dioxide | cut-off, U], 0.488 kg of manganese(III) oxide [manganese(III) oxide {GLO}| market for manganese(III) oxide | cut-off, U], and 0.404 kg of water [water, deionized {Europe without Switzerland}| market for water, deionized | cut-off, U]
- 1 kg of strontium nitrate is modeled as: 0.597 kg of strontium carbonate [strontium carbonate, 95%, at plant/GLO S], and nitric acid [nitric acid, 50% in H_2O, at plant/US-US-EI U]

Appendix E: Syngas Fermentation to Ethanol and Ethanol Separation

Syngas fermentation is considered a route for upgrading syngas to alcohols, with the primary intention of focusing on ethanol production. A range of reaction schemes are proposed in the literature for syngas fermentation, with the exact route influenced by factors such as microbes and enzymes used, and the gas composition of the feed. The most broadly referenced of these is the Wood–Ljungdahl pathway which covers the production of acetogens and their end products (e.g., ethanol, acetate, butanol, butyrate).

The approach taken to fermentation within this assessment treats the unit itself as a black box with a simplified reaction scheme focusing on the production of ethanol and acetate (specifically in the form of acetic acid) as a by-product.

Two inventories are listed, one for a standard SOEC conversion, and one for the advanced (both utilizing the biomass heat route)—both inventories use the "advanced" PEM electrolyzer model.

The following generalized scheme is considered, provided in Phillips et al. [31]

Acetic Acid

$$CO + CO_2 + \left(nCO + \left(3-n\right)H_2\right) \rightarrow CH_3COOH + nCO_2 + \left(1-n\right)H_2O$$

where n can be values between $3 \geq n \geq -1$.

Ethanol

$$CO + CO_2 + \left(nCO + \left(5-n\right)H_2\right) \rightarrow CH_3CH_2OH + nCO_2 + \left(2-n\right)H_2O$$

where n can be values between $5 \geq n \geq -1$. A minus number on the right-hand side of the equation means that the material is being consumed rather than produced.

Acetic acid is considered a by-product and is not assigned any of the impacts associated with the production of ethanol.

Here, an approach similar to that used in Biermann et al. [46] and Pardo-Planas et al. [47], where four reactions are considered for ethanol production included in Table E.1. The table also includes a "conversion ratio"—addressing the balance of the rate of each reaction. This ratio was adapted from data in the Biermann et al. source. Pardo-Planas et al. detailed a simulation of a gasifier acting as a source of syngas for a fermenter. The article concludes that the conversion rate of both gases is impactful on the overall energy balance of the plant, investigating conversion ratios of both gases up to 95%. A compilation of data is shown in Tables E.1 and E.2.

H_2 is only added to convert any CO_2 present to ethanol and should only be added if the conversion is assumed to be sufficiently high that energetically and economically makes sense. It is assumed that only 50% of the CO_2 in the feed is reacted.

This model assumes a 90% conversion of both CO and H_2—with the remaining unreacted gases combusted before release. 5% of the product is assumed to be acetate that will be removed during distillation and returned or purged.

TABLE E.1 Key summary reactions for CO and CO_2 fermentation.

Reaction	Base component	Conversion ratio
$6CO + 3H_2O \rightarrow C_2H_6O + 4CO_2$	CO	10
$4CO + 2H_2O \rightarrow 2CO_2 + CH_3COOH$	CO	1
$2CO_2 + 4H_2 \rightarrow 2H_2O + CH_3COOH$	H_2	1
$2CO_2 + 6H_2 \rightarrow C_2H_6O + 3H_2O$	H_2	28

TABLE E.2 Inventories for ethanol synthesis from syngas fermentation with separation process.

Component	Unit	Scenario	
		Standard	Advanced
Outputs			
Ethanol	kg	1	1
Acetic acid	kg	0.05	0.05
Inputs			
Tap water	L	5	5
CO from SOEC	kg	2.029	3.364
CO_2 from SOEC (for reaction)	kg	0.957	0.327
H_2 from PEM	kg	0.145	0.05
Nutrients	g	8	8
Heat from waste, at municipal waste incineration plant/US*US-EI U	MJ	3	3
Electricity, at wind power plant 800 kW/US-US-EI U	kWh	0.2	0.2

Appendix F: Fischer–Tropsch Conversion with Reverse Water–Gas Shift

Data on energy and product mix were taken from the literature [40] with additional information for catalysts and water usage collected separately [41]. A compilation is provided in Table F.1.

Appendix G: Technology Maturity Assessment

The selection of processes within the system reflects the goal to assess at or close to market technologies, while a more detailed assessment is considered in the relevant subsection of the inventory and impact assessment (Table G.1).

TABLE F.1 Product mix for Fischer–Tropsch conversion with RWGS and required inputs.

Outputs	Qty.	Unit
Kerosene for SAF	1	kg
Naphtha	0.55	kg
Diesel	0.59	kg
Inputs	**Qty.**	**Unit**
Carbon dioxide, in air, biogenic	14.54	kg
Water, cooling, unspecified natural origin, US	19.9	L
Hydrogen, PEM electrolysis—future energy consumption	1.36	kg
Water, completely softened, at plant/US-US-EI U	32.79	kg
Cobalt, at plant/GLO US-EI U	0.002	kg
Nickel, 99.5%, at plant/GLO US-EI U	6.44E−05	kg
Zeolite, powder {GLO}| market for zeolite, powder | cut-off, U	3.50E−05	kg
Electricity, at wind power plant 800 kW/US-US-EI U	0.528	kWh

TABLE G.1 Summary of maturity assessment for technology selection.

Process	Maturity Assessment
Corn production	Both corn cultivation and the fermentation of corn to produce bioethanol are mature, at-scale processes
Bioethanol fermentation	
Alcohol to jet conversion	Emerging technology, a FOAK bioethanol to jet fuel plant constructed in the US (Freedom Pines Plat operated by LanzaJet)
PEM electrolysis for H_2 production	Emerging technology, with a transition away from FOAK plants to larger-scale production. IEA figures show a total installed capacity of 217 MW in 2022, with this estimated to grow to 921 MW in 2023. The same source shows a total installed capacity of all electrolyzer types of 687 MW in 2022, with this expected to grow to 2884 MW in 2023. IEA also highlights that if all projects in the existing pipeline are realized by 2030, total installed capacity could reach 170–365 GW
High-temperature SOEC for CO production	Emerging technology, Haldor Topsoe sells the eCOS™ unit, which is a high-temperature solid oxide electrolyzer to produce high-purity carbon monoxide
Syngas fermentation	Emerging technology, LanzaTech operates microbial reactors that convert carbon monoxide to ethanol, with ongoing projects to develop processes that can also utilize carbon dioxide
Reverse water–gas shift (RWGS) for syngas production	Emerging technology, Notable developments include: The Shell and MAN Energy Solutions RWGS pilot, which has been running since early 2023 and the Johnson Matthey HyCOgen technology, and the Norske fuels "Project Mosjøen" will utilize a RWGS to produce syngas when constructed
Fischer–Tropsch conversion	FT conversion of syngas is an established technology for the production of a broad range of hydrocarbon fuels and petrochemical feedstocks, efforts to optimize output production for maximum SAF or syncrude output are ongoing. The proposed DG fuels plant in Louisiana will use the Johnson Matthey FT CANS™ technology that converts syngas to syncrude. Johnson Matthey stated that the combined HyCOgen and FT CANS technologies can convert over 95% of the input CO_2 into syncrude (SAF to diesel and gasoline ratio not specified) The combined HyCOgen and FT CANS technology is to be used for synthetic fuel production at the Aramco and Repsol plant in Bilbao (due to be commissioned in 2024 with a starting capacity of 2100 tpa), a large deployment of the FT CANS technology is also planned for the DG fuels proposed project in Louisiana

Appendix H: Uncertainty Assessment Data

Table H.1 shows a compilation of scores for five categories (reliability, completeness, temporal correlation, geographical correlation, and further technological correlation).

TABLE H.1 Uncertainty assessment covering major technologies/inventories with calculated uncertainty factor (SD_{g95}).

Technology	Pedigree matrix assessment	Calculated SD_{g95}	Details
PEM for H_2 production	(3,4,3,3,2)	1.2	As shown in inventory section and the appendices, this is an estimate based on literature data
HT-SOEC for CO production	(4,4,2,3,2)	1.25	As shown in inventory section and the appendices, this is an estimate based on literature data and some additional process modeling by the authors
RWGS-FTS	(3,4,3,2,2)	1.2	As shown in inventory section and the appendices, this is an estimate based on literature data
FTS standalone	(3,4,2,2,2)	1.17	As shown in inventory section and the appendices, this is an estimate based on literature data
Syngas fermentation	(4,4,2,2,2)	1.25	As shown in inventory section and the appendices, this is an estimate based on literature data and some additional process modeling by the authors
ATJ	(3,4,2,2,2)	1.17	As shown in inventory section and the appendices, this is an estimate based on literature data
Heat pump for corn drying	(4,4,3,2,2)	1.27	As shown in inventory section and the appendices, this is an estimate based on literature data